Desalination and Water Treatment
www.deswater.com

doi: 10.5004/dwt.2018.22372

121 (2018) 92–103
July

Removal and recovery of thorium from aqueous solution using new polyurethane bearing azomethine and urethane chelators: kinetics, thermodynamics, and isotherm analysis

Rajagopal Mahalakshmi[a,b], Selvaraj Dinesh Kirupha[c], Kumarasamy Rathina[a,b], Lingam Ravikumar[d,e,*]

[a]*Research and Development centre, Bharathiar University, Coimbatore, India, Tel. +91-9843776968; email: mahalnet@gmail.com (R. Mahalakshmi), Tel. +91-9841567590; email: rathina.k.sci@kct.ac.in (K. Rathina)*
[b]*Department of Chemistry, Kumaraguru College of Technology, Coimbatore, India*
[c]*Department of Chemistry, Coimbatore Institute of Technology, Coimbatore, India, Tel. +91-9597091915; email: dineshf086@gmail.com (S.D. Kirupha)*
[d]*Research and Development centre, Bharathiar University, Coimbatore, India, Tel. +91-9442370098; email: ravikumarcbm@rediffmail.com (L. Ravikumar)*
[e]*Department of Chemistry, CBM College of Arts and Science, Coimbatore, India*

Received 26 February 2018; Accepted 8 April 2018

ABSTRACT

A conventional condensation polymerization was adopted to prepare a new polyurethane (PoU) using dialdehyde monomer and methylene diisocyanate (MDI) in dimethylformamide (DMF) solvent. The synthesis and structure of the PoU polymer was confirmed by Fourier transform infrared spectroscopy (FTIR), proton nuclear magnetic resonance (^{1}H-NMR), scanning electron microscopy (SEM), and energy dispersive X-ray (EDX) analysis spectral studies. The synthesized PoU resin was tested as an adsorbent using batch-mode adsorption experiments for the removal and recovery of Th(IV) ion. Maximum Th(IV) removal of 89.3% was observed at optimized pH value of 5.0, using 40 mg/L of initial metal ion concentration with equilibrium time of 60 min. From the kinetic studies, it was observed that the adsorption reaction follows pseudo-second-order kinetic model, suggesting that more than one interaction involves in the rate determining step. From thermodynamic studies, enthalpy ($\Delta H°$), entropy ($\Delta S°$), Gibbs free energy ($\Delta G°$), and activation energy (E_a) were calculated, and the process is found to be exothermic and spontaneous. The reusability studies showed that 0.1 M HCl can effectively desorb the absorbed Th(IV) ion within 60 min, and the PoU resin was found to be effective up to five cycles depicting its stability nature.

Keywords: Polyurethane; Thorium removal; Nonlinear modeling; Reusable; Adsorption mechanism

1. Introduction

Increased knowledge about the ecotoxicological effects of radiotoxic pollutants, environmental disquiets related to disposal and increased legal constraint in the reduction of industrial emission from radionuclide wastewater source necessitate research and development in the area of wastewater treatment [1,2]. When the radiotoxic pollutant thorium enters the water stream, thorium ion gets hydrolyzed into insoluble hydroxides as $Th(OH)_2^{2+}$, $Th(OH)^{3+}$, $Th_2(OH)_2^{6+}$, and $Th_6(OH)_5^{9+}$ and gets accumulated [3]. Presence of various

* Corresponding author.

Presented at the 3rd International Conference on Recent Advancements in Chemical, Environmental and Energy Engineering, 15–16 February, Chennai, India, 2018.

forms of radiotoxic metals even in the trace level in the environment can cause health issues such as lung, pancreatic, and liver cancers due to the accumulation of thorium as hydroxide in human tissue, liver, spleen, and marrow [4]. Thorium is an actinide element found in tetravalent state and present in natural sediments in minerals such as monazite, rutile, and thorianite [5]. Thorium is mainly used in the applications of aeronautics and aerospace, optics, radio, metallurgy and chemical industry, nuclear industry, and material field. Thorium is considered to be an important fuel for running nuclear breeder reactors, by converting thorium into 233U [6]. According to the WHO and U.S. protection agency guidelines, the maximum permissible discharge level of uranium from industries should be between the range of 0.1 and 0.5 mg/L and the concentration of uranium and thorium in drinking water should be below 0.01–0.03 mg/L [7,8]. Because the presence of long-lived radionuclides significantly increases the complexity in the waste aqueous system, an accurate estimation of uranium concentration from radionuclide wastewater is necessary, and on the other hand, cost of recovery of such radionuclides are predominantly high so an effective separation process is needed for recovering such radionuclides from industrial wastewater before entering the living environment. Some of the conventional techniques used so far for the extraction of heavy metal ions are chemical precipitation, solvent extraction, membrane separation, reverse osmosis, coagulation, electrofloatation, ion exchange, and sorption process [9–11]. The most convenient and effective method for the separation of trace amount of toxic heavy metals from large volume of contaminated wastewater is adsorption technique [12]. The main advantages in adsorption technique are simplicity in design, ease of operation, convenience in process operation, and effective trace amount removal resulted adsorption method as superior among other techniques [13,14]. The main criteria to be considered while choosing an adsorbent in the process are separability, cost-effectiveness, and adsorption capacity [15]. Based on these criteria, many adsorbents were reported for thorium removal from contaminated aqueous systems such as perlite [6], PAN-zeolite composite [16], alumina [17], carbon [18], bentonite [19], molecular sieves 13-X [20], and 4-vinyl pyridine-based hydrogels [21], etc. Apart from these factors, the critical factor which determines the maximum recovery of toxic metals in the adsorption technique is by choosing a suitable chelating agent with good stability nature [22]. O-vaniline semicarbazone-Amberlite XAD-4 (Polystyrene-divinyl benzene copolymer) [23], quinoline-8-ol cellulose [24], activated carbon [18], calix[4]arene-o-vanillinsemicarbazone-styrene-divinyl benzene (SDB) [25], N,N′-dimethyl-N,N′-dibutylmalonamide-SDB [26], and G3-poly(amido) amine dendron-SDB [2] were adsorbents having selective chelating functional groups impregnated on the surface of the resin used for the removal of radionuclides reported. This work is designed with reference to our previous work, synthetic polymers bearing donor atoms used for the removal of toxic metal ions (d-block) from industrial effluents [27–29].

In this study, we have synthesized a polyurethane (PoU) resin with chelating functional group which can effectively take part in the removal of thorium from wastewater through batch adsorption study. Experiment parameters such as solution pH, adsorbent dose, initial thorium metal ion concentration, and contact time were optimized. Adsorption isotherms were analyzed with Langmuir, Freundlich, Sips, and Temkin isotherm models to find the rate limiting step of the adsorption process. Influences of temperature predicting the nature of the reaction were studied. Pseudo-first-order, pseudo-second–order, and intraparticle diffusion kinetic models were plotted with experimental data to find out the rate of the reaction and mechanism involving in the adsorption process. Desorption studies were performed with different eluting agents to test the chemical stability and the efficiency of the PoU adsorbent.

2. Experimental details

2.1. Materials required

2,4-dihydroxybenzaldhyde (Sigma-Aldrich, Germany), *p*-aminobenzoic acid (Sigma-Aldrich), and methylene diisocyanate (MDI) (Sigma-Aldrich) were purchased and used as such. Dimethylformamide (DMF) was distilled using CaS_2 for 72 h, distilled under reduced pressure, and stored dry. Absolute ethanol was refluxed with calcium chloride, distilled, and stored dry. All other reagents used in the synthesis and batch equilibrium experiments were of analytical grade.

2.2. Synthesis of 2′,4′-dihydroxybenzaniline-4-carboxylic acid monomer

2,4-dihydroxy benzaldehyde (1 mol) was condensed with *p*-amino acid benzoic acid (1 mol) in a Dean–Stark apparatus for 15 min in acidic medium and refluxed slowly in an oil bath for 6 h. The azeotropic mixture was removed, and the resulting slurry was collected. After completion of reaction, the monomer was filtered, washed several times with water and finally with absolute ethanol, and dried under vacuum for 3 h. The synthesis scheme of 2′,4′-dihydroxybenzaniline-4-carboxylic acid (DHBACA) monomer is presented in Fig. 1.

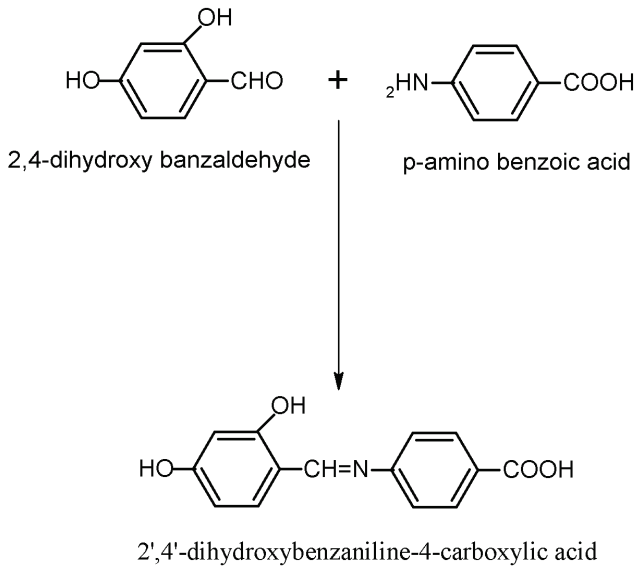

Fig. 1. Synthesis of 2′,4′-dihydroxybenzaniline-4-carboxylic acid (DHBACA) monomer.

2.3. Synthesis of PoU

The synthesis scheme of PoU is presented in Fig. 2. To DHBACA monomer (1 mol), MDI (1 mol) was slowly added and magnetically stirred with DMF medium at room temperature for 30 min. with DABCO catalyst. The temperature was then slowly raised to 90°C and refluxed for 6 h. After completion of the reaction, the mixture was poured into water. The precipitated polymer so formed was filtered and washed with dilute HCl, water, and finally with absolute ethanol.

2.4. Characterization techniques

The synthesized DHBACA monomer and the PoU polymer were characterized using proton nuclear magnetic resonance (^{1}H-NMR) spectra at 100.52 MHz on a Bruker AMX-200 spectrometer. Fourier transformation infrared analysis was performed using Shimadzu spectrophotometer with KBr pellets. The surface area of the synthesized PoU polymeric resin and thorium adsorbed PoU were analyzed using LEO Gemini 1530 scanning electron microscope (SEM) and energy dispersive X-ray (EDX) spectrometry using Bruker AXS microanalysis GmbH on a dry sample. Systronic microprocessor pH meter (μ-362) used for pH measurements. UV-Vis double beam spectrophotometer, Shimadzu UV-1800, was used in the determination of Th(IV) ion concentration.

2.5. Preparation of thorium stock solution

Thorium stock solution was prepared using thorium nitrate hexahydrate ($Th[NO_3]_4.6H_2O$) purchased from BDH Chemicals, India. A total of 1 M of ammonium acetate buffer solution was prepared by dissolving ammonium acetate in distilled water. The pH was adjusted to 3.3 with 3 M HCl, and the volume was made up to 1 L with distilled water. The batch equilibrium experiments were conducted using distilled water purified using standard procedure. Arsenazo III (0.15% w/v; aq.) was prepared using (2,2′[1,8-dihydroxy-3,6-disulfo-2,7-napthalene-bis{azo}]dibenzenearsonic acid) (BDH Chemicals) with distilled water. The solution was allowed to stand for 1 h and then filtered to remove residual solid.

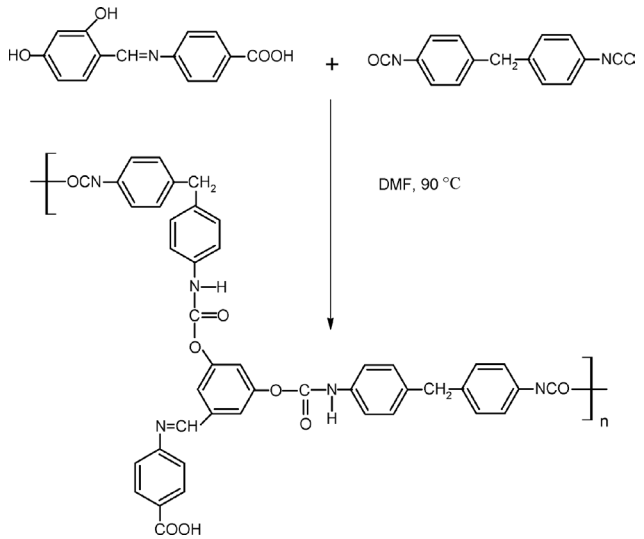

Fig. 2. Synthesis of polyurethane (PoU).

2.6. Batch adsorption experiment

Batch adsorption experiments were conducted using 20 mL of Th(IV) metal solution containing 40 mg of the PoU resin in a conical flask, placed in a orbital bench shaker for 60 min, agitated at 200 rpm to achieve equilibrium, and the samples were centrifuged at 2,000 rpm. The residual Th(IV) ion concentration was determined by means of UV-Vis spectrophotometer at 660 nm with the help of arsenazo, as chromogenic agent. The pH of the solution was adjusted from 2 to 8 using 0.1 M of NaOH and 0.1 M of HCl with initial metal solution of 10 mg/L concentration. The pH of the Th(IV) solution was checked before analyzing every parameter and adjusted to initial value. To measure the cost-effectiveness of the system, the volume of adsorbent was varied from 10 to 60 mg in 20 mL of 10 mg/L Th(IV) ion solution at 30°C. With concentration ranging between 10 and 50 mg/L of Th(IV) solutions were used for isotherm studies. The initial concentration and the final concentration of Th(IV) ion after every experiment trail were analyzed using UV-Vis spectrophotometer. The percentage of thorium removal is calculated using Eq. (1):

$$\% \text{ Th(IV) removal} = \frac{C_i - C_f}{C_i} \times 100 \quad (1)$$

The adsorption capacity (q_e) of the PoU is calculated using the mass balance relation:

$$q_e = \frac{(C_i - C_f)V}{m} \quad (2)$$

where C_i and C_f are the initial and final thorium concentrations of the solution before and after adsorption, respectively, V is the volume of the solution taken for the adsorption study, and m is the mass of the adsorbent. For each experiment, an average of three replicates was done to minimize the error with standard deviation of 2%. If the error percentage increases, the solution was discarded, and the experiments were repeated again until the standard error is under the acceptable limit.

The isotherm data were plotted using nonlinear method with MATLAB 7.1 version. The variable and parameter constants obtained were compared with the experimental results to find out the best isotherm fit and kinetic model which predicts the reaction rate and pathway of the adsorption experiment.

3. Results and discussion

3.1. Characterization and PoU resin

The Fourier transform infrared spectroscopy (FTIR) spectrum of PoU resin (Fig. 3) shows the –NH stretching frequency of urethane link and that of –OH stretching frequency

of pendent –COOH groups as a broad band at 3,317 cm^{-1}. The amide carbonyl stretching frequency of urethane link was observed as a broad band around 1,666 cm^{-1} [30]. The –N=CH– stretching frequency appeared at 1,597 cm^{-1}. The H–N–C=O amide-II frequency appeared at 1,519 cm^{-1}. This confirms the synthetic polymeric resin is PoU with azomethine moiety [31,32]. ^{1}H-NMR spectrum of PoU (Fig. 4) shows the hydrogen of –COOH group appeared at δ = 10.0 ppm. A signal at δ = 9.7 ppm is due to the hydrogen of the amide link. The azomethine protons appeared at a δ value of 8.5 ppm. The aromatic hydrogen of the polymer appeared between δ = 7.5 and 7.0 ppm. The methylene between aromatic rings appeared at δ = 2.5 ppm. These observations support the formation of the adsorbent having chelating groups which can form complexes with metal ions.

Surface morphology of the raw and Th(IV) adsorbed PoU resin were studied using SEM micrographs shown in Figs. 5(A)–(D). From the SEM image of the raw PoU resin (Fig. 5(A)), it was clear that the surface is nonparticulate and abundant in folds. The dry surface of the polymer matrix shows numerous irregularities that increase the contact area with the metal solution and improve the metal adsorption. The SEM micrograph Th(IV) adsorbed PoU resin (Fig. 5(B)) showed agglomeration of Th(IV) ions into the pores and surface of the PoU resin which are clearly visible through formation of dark patches around white spots. The EDX analysis of raw PoU (Fig. 5(C)) clearly showed the presence of C, N, and O atoms alone. But Th(IV)-loaded PoU resin (Fig. 5(D)) showed the presence of C, N, and O along with Th(IV) atoms justifying the adsorption of Th(IV) ion by the PoU resin.

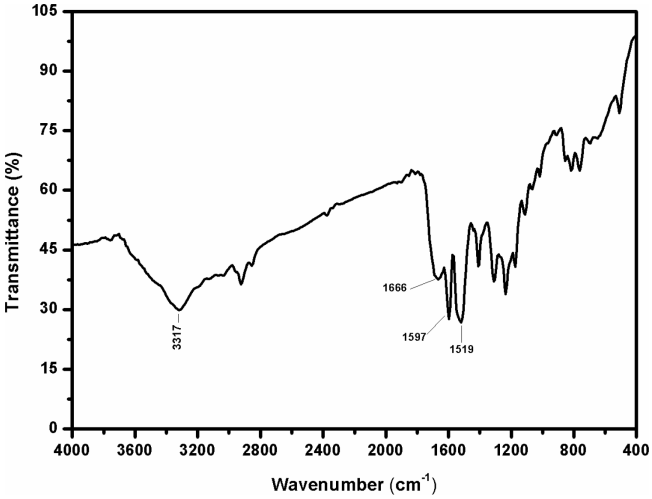

Fig. 3. FTIR spectrum of polyurethane PoU.

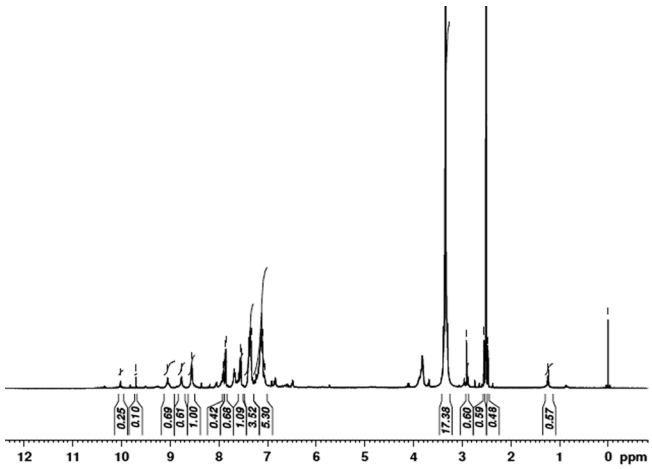

Fig. 4. ^{1}H-NMR spectrum of polyurethane PoU.

3.2. Effects of pH onto Th(IV) adsorption

Solution pH is one of the most important parameters which signifies the effect of protonation and deprotonation of the adsorbent, metal speciation, surface metal binding sites, and adsorbate functional groups. The effect of initial pH values on the adsorption efficiency of Th(IV) ion removal by PoU polymeric resin was investigated, and the results were shown in Fig. 6. The adsorption capacity increased with the increase of the pH values, and the maximum metal uptake was obtained at pH 6 for the Th(IV) ions. Any further increases in the pH value have not resulted in any increase of Th(IV) ions, and the adsorption capacity remained almost constant up to a pH value of 8. Because the chelating sites are weakly basic and had good affinity for H^+, and at lower pH values the PoU resin is partially hydrolyzed, and there was a competitive adsorption between metal ions and H^+, they have resulted in lower metal ion adsorption capacities at the pH range of 2–3. Because Th(IV) ion adsorption dominates in acidic pH, conforming the process is ion-exchange with replacement of hydrogen ions from the weakly acidic carboxyl group and the amide group present in the polymeric chain. Hence, between the pH range of 4 and 6, the hydrogen ions present in the carboxyl and amide chelating group gets deprotonated, resulting in increase in negative binding sites which are more favorable and effective adsorption pathway [33–36].

3.3. Effect of adsorbent dose and initial Th(IV) concentration onto Th(IV) adsorption

The effect of the solid/liquid ratio (10–60 mg) on Th(IV) ion adsorption at 30°C at an initial pH 6.0 was investigated, and the results were presented in Fig. 7. At the initial stage, increase in adsorption was due to the amount of solid/liquid ratio increase. The available adsorbing site present in the adsorbent surface results in the increase in adsorption capacity was noticed [37–39]. Maximum removal of 88% was achieved with 40 mg of the PoU resin, and thereafter, increase in Th(IV) removal was almost constant above the solid/liquid ratio of 40 mg. Hence, under economical conditions, the optimized solid/liquid ratio was fixed as 40 mg for further adsorption experiments. The experimental results with effect of Th(IV) concentration on Th(IV) removal was shown in Fig. 7. The plot showed that with increase in Th(IV) ion concentration (10–60 mg/L), the adsorption capacity increases gradually, this is mainly due to the higher adsorption rate and consumption of active sites present in the PoU adsorbent by the metal ions with increase in concentration [40–43].

3.4. Effects of contact time onto Th(IV) adsorption

To test the design, modeling of the batch reactor, and prediction of adsorption rate, adsorption experiments were

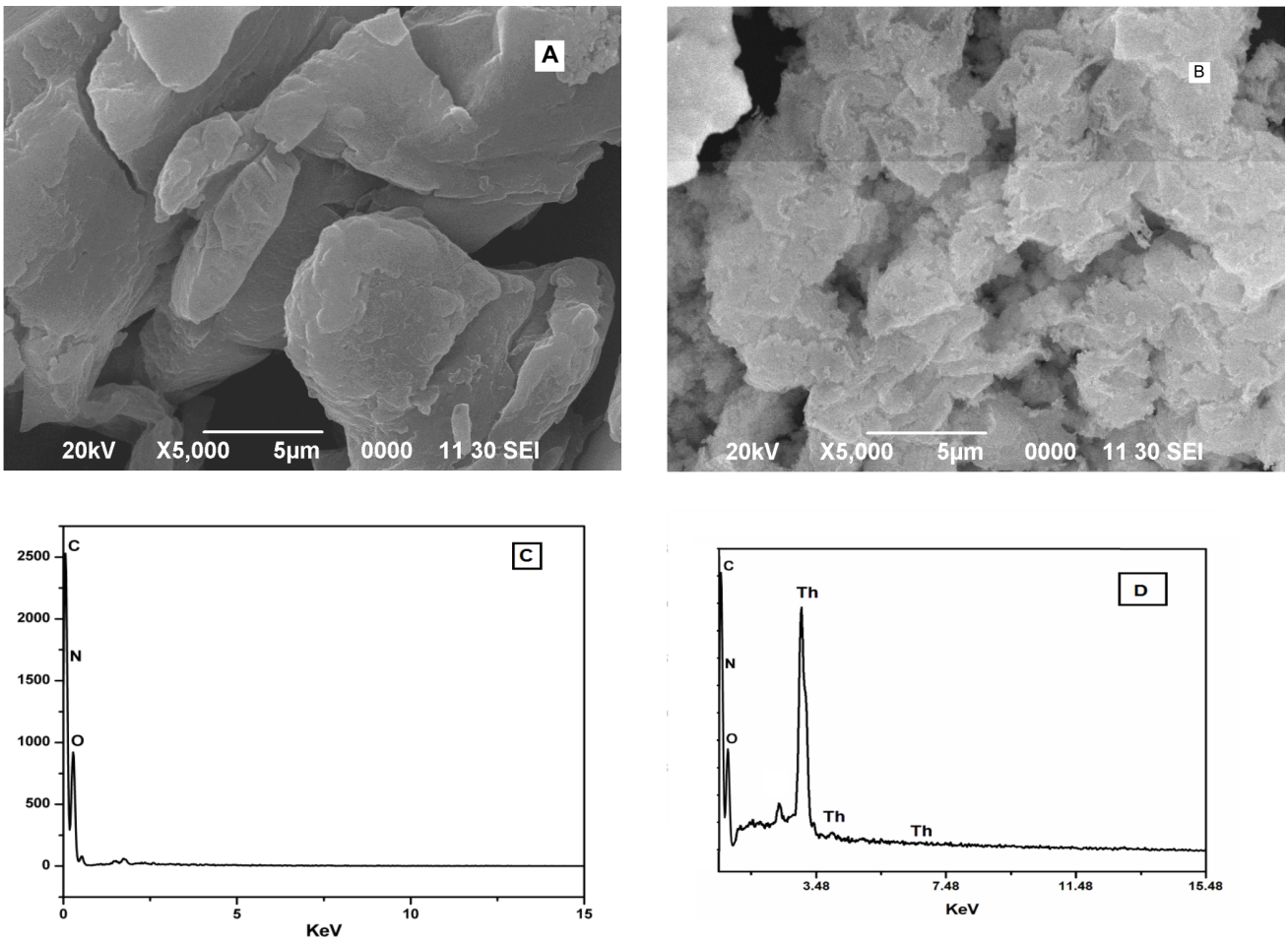

Fig. 5. SEM micrographs of raw and Th(IV)-adsorbed PoU resins: (A) SEM micrograph of raw PoU resin, (B) SEM micrograph of Th(IV) metal–adsorbed PoU resin, (C) EDX analysis of raw PoU resin, and (D) EDX analysis of Th(IV)-adsorbed PoU resin.

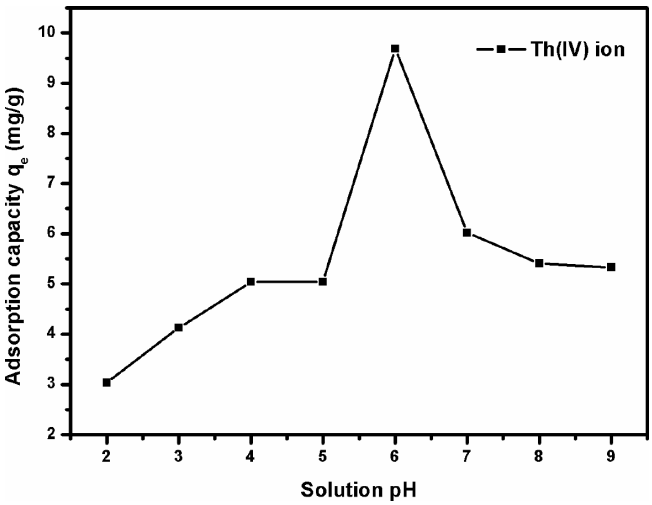

Fig. 6. Effect of pH onto Th(IV) ion sorption using PoU adsorbent (initial thorium ion concentration, 10 mg/L; adsorbent dose, 20 mg/L; and contact time, 60 min).

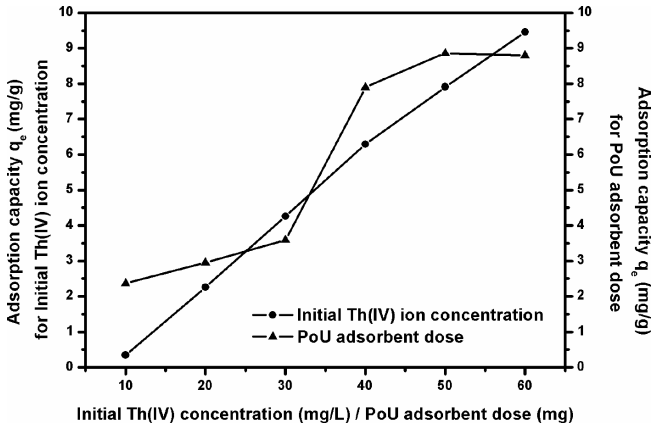

Fig. 7. Effect of PoU adsorbent dose onto Th(IV) ion sorption (initial thorium ion concentration, 10 mg/L; pH, 6; contact time, 60 min) and effect of initial Th(IV) ion concentration onto Th(IV) adsorption using PoU adsorbent (pH, 6; PoU dose, 40 mg; and contact time, 60 min).

conducted under optimized conditions with initial thorium metal ion concentration (50 mg/L); the contact time with the adsorbent was investigated up to 60 min with 10 min time interval, and the results are presented in Fig. 8. The thorium removal was rapid initially for 20 min and slowly reaches a saturation point 60 min. The initial rapid phase is due to the availability of more number of adsorption sites on the surface

of the PoU adsorbent [44–47]. Any increase in the time after the equilibrium time showed no change in the removal of Th(IV) ions.

3.5. Adsorption kinetics

A kinetic model is an important tool in determining the operating parameters to run a full-scale batch-mode reactor. Pseudo-first-order model [48–50] from Legergren (Eq. (3)) is often used for the estimation of k_1 and mass transfer coefficient in the adsorption process design. The linear form of pseudo-first-order model is as follows:

$$\log(q_e - q_t) = \log q_e - \frac{K_{ad}}{2.303} t \quad (3)$$

where q_t is the amount of thorium ion adsorbed by the PoU adsorbent at time t (mg/g), and k_{ad} (min^{-1}) is the rate constant of pseudo-first-order kinetic model. A graph was plotted for pseudo-first-order kinetic model with obtained experimental values with time t (min.) against $\log(q_e - q_t)$ in Fig. 9 and the kinetic parameters and the values calculated were tabulated (Table 1). The corelation coefficient obtained from pseudo-first-order kinetic model was found to be low. Pseudo-second-order model by Ho and Mckay [51,52] describes about the amount of metal adsorbed at equilibrium and amount of metal adsorbed onto the surface of the adsorbent. It depends directly on the rate of adsorption onto the adsorbent active sites (Eq. (4)). The linear form of pseudo-second-order model is as follows:

$$\frac{t}{q_t} = \frac{1}{kq_e^2} + \frac{1}{q_e} t \quad (4)$$

K (g/mg.min) is the rate constant of pseudo-second-order kinetic model. A plot of t/q_t versus t (Fig. 9) should give a straight line if pseudo-second-order kinetic model is applicable. The correlation coefficient found to be high (>0.99). When the experimental and calculated q_e values were compared, it was found to be almost similar (Table 1). These observations suggest that the adsorption of Th(IV) onto PoU adsorbent

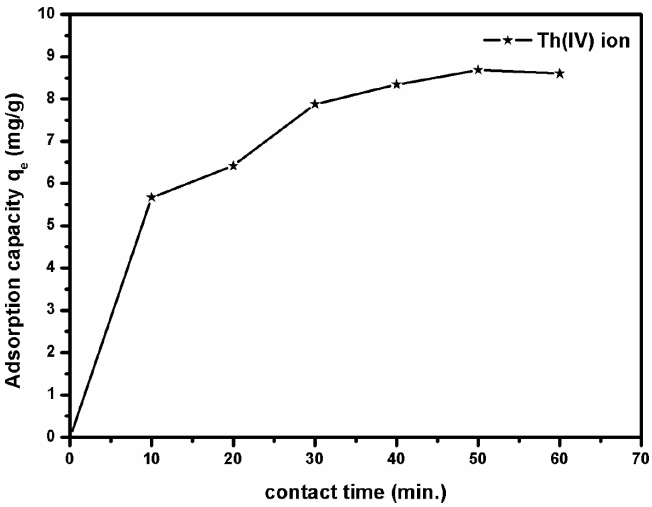

Fig. 8. Effect of contact time onto Th(IV) ion sorption using PoU adsorbent (adsorbent dose, 40 mg/L; pH, 6; and initial thorium ion concentration, 10 mg/L).

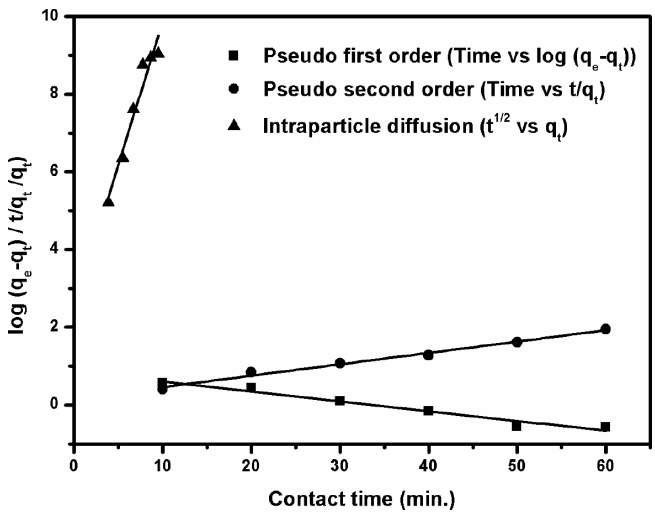

Fig. 9. Kinetic models of PoU adsorbent onto Th(IV) removal at 30°C.

Table 1
Kinetic parameters and constants for Th(IV) removal by PoU adsorbent

Adsorption kinetic model		Parameters and constants for Th(IV) removal
Pseudo-first-order kinetic model	K_{ad} (min^{-1})	0.055
	q_e (mg.g^{-1})	1.43
	R^2	0.9650
Pseudo-second-order kinetic model	K (g.mg^{-1}.min^{-1})	0.0082
	q_e, predicted (mg.g^{-1})	10.75
	h (mg.g^{-1}.min^{-1})	0.96
	q_e, experimental (mg.g^{-1})	8.91
	R^2	0.9950
Intraparticle diffusion model	K_p (mg.g^{-1}.min$^{-0.5}$)	0.839
	C	2.85
	R^2	0.9510

follows pseudo-second-order kinetic model with chemisorptions as the rate-limiting step.

Intraparticle diffusion model given by Weber and Morris [53] (Eq. 5) is used to verify the influence of mass transfer resistance of binding of metal ions onto PoU adsorbent, if the rate determining step is chemisorption.

$$q_t = k_p t^{1/2} + C \tag{5}$$

where C is the intercept and K_p is the intraparticle rate constant (mg/g.min$^{1/2}$). Intraparticle diffusion model describes about the control of mass transfer resistance on the binding of Th(IV) onto PoU resin. Due to the adsorption capacity varying nature in the initial and final stage of the adsorption experiment, there exhibits the curve with dual nature. This can be attributed due to the fact that the initial part (intercept region) of the adsorption is due to the boundary layer outcome and in the later part (linear curve region) is due to the intraparticle diffusion outcome. When the plot of q_t against $t^{1/2}$ was constructed from the obtained experimental results (Fig. 9), the slope should be linear and should pass through the origin, showing that intraparticle diffusion model is the sole rate-limiting step. The larger is the intercept, the greater is the influence as rate-controlling step with the adsorption on the surface of the adsorbent. Because the linear plot does not pass through the origin suggesting that the intraparticle diffusion model does not plays the sole rate-limiting step in constructing the design of the experiment, it has some influence in the adsorption design.

3.6. Adsorption isotherms

The function of the adsorption isotherm is to narrate the adsorbate concentration in the bulk solution and the amount of thorium ion adsorbed in the solid/liquid phase. When the experimental data on the effect of initial thorium ion concentration against the surface of the PoU adsorbent was taken and fitted using MATLAB 7.1. The nonlinear form of Langmuir [54], Freundlich [55], Sips [56], and Temkin [57] isotherms are used to describe the adsorption isotherm in the system. The graphical representations of the isotherm models fitted with experimental results were presented in Fig. 10.

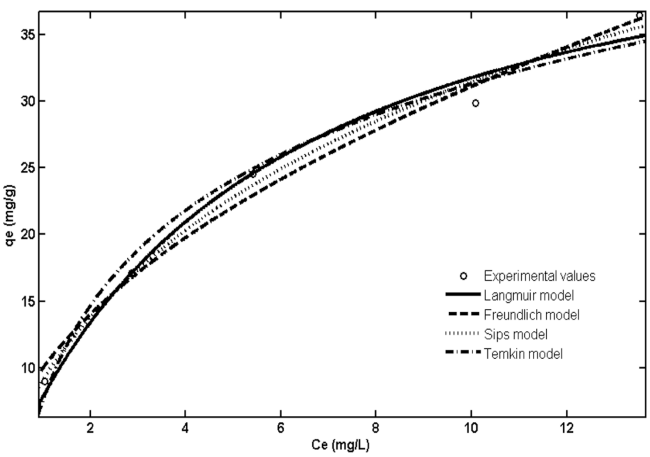

Fig. 10. Nonlinear adsorption isotherm model for Th(IV) removal using PoU adsorbent.

The parameter values and constants obtained are tabulated (Table 2). The nonlinear form of Langmuir isotherm (Eq. (6)) is as follows:

$$q_e = \frac{q_m K_L C_e}{1 + K_L C_e} \tag{6}$$

where q_m (mg/g) is the Langmuir constant and K_L is the amount of solute required for the unit mass of the adsorbent for the monolayer coverage on the surface of the adsorbent and the heat of adsorption, respectively. Langmuir isotherm describes about the homogeneous monolayer formation, equivalent surface sites, and interactions between the adsorbed molecules. The Langmuir adsorption constant q_e (mg/g) and K_L discusses about the amount of solute adsorbed per unit mass of the adsorbent required for the monolayer of adsorption and heat of adsorption, respectively. The maximum monolayer adsorption capacity obtained was found to be 48.4 mg/g for PoU. The predominant factor in Langmuir isotherm parameters can be used to predict the binding affinity between the adsorbate and the adsorbent using a dimensionless equilibrium parameter "R_L" expressed as follows:

$$R_L = \frac{1}{1 + K_L C_o} \tag{7}$$

where K_L is the Langmuir constant and C_o is the initial thorium ion concentration. The value of separation parameter R_L provides important information about the nature of

Table 2
Parameters and isotherm constants of Th(IV) removal using PoU adsorbent through nonlinear method

Adsorption kinetic model		Parameters and constants for Th(IV) removal
Langmuir model	q_m (mg.g^{-1})	4.84
	K_L (L.mg^{-1})	0.1909
	R^2	0.9845
	SSE	7.15
Freundlich model	K_F [(mg.g^{-1})(L.mg^{-1})(n^{-1})]	9.93
	n (g.L^{-1})	2.01
	R^2	0.9868
	SSE	6.12
Sips model	Q_s (mg.g^{-1})	10.23
	K_S (L.g^{-1})	0.713
	n_s	0.0581
	R_s	0.6698
	R^2	0.9902
	SSE	4.52
Temkin model	B	2.05
	A	4.49
	R^2	0.9735
	SSE	9.20

adsorption. The value of R_L indicates the type of Langmuir isotherm to be irreversible ($R_L = 0$), favorable ($0 < R_L < 1$), linear ($R_L = 1$), or unfavorable ($R_L > 1$) [58]. The R_L value was found to be 0.094, in the range of 0–1 for 50 mg/L of initial Th(IV) ion concentration indicating favorable adsorption.

Freundlich isotherm describes well in detail about the type of adsorption process. It mainly indicates the type of adsorption on the heterogeneous surface which fits with the wide range of concentration. The Freundlich equation also proposes that the sorption energy exponentially decreases with completion of sorptional active center of the adsorbent species:

$$\text{Freundlich isotherm}: q_e = K_F C_e^{1/n} \tag{8}$$

where K_F (1/g) is the Fruendlich constants signifying about the adsorption intensity and bonding energy and n is the heterogeneity factor. The n value indicates the degree of nonlinearity between the adsorption process and solution concentration. If the adsorption process is linear ($n = 1$), chemisorption ($n < 1$), physisorption ($n > 1$) [59]. The value of n was found to be 2.01 for PoU. Because the value of n is ($1 < n < 10$), it indicates the adsorption is favorable.

Sips isotherm (Eq. (9)) is the combination of Langmuir and Freundlich isotherms which elucidates about the physical and chemical characterization of adsorption. It suggests the monolayer formation of Langmuir isotherm, at higher adsorbate concentration. It gets reduced to Freundlich isotherm, at lower concentration respectively. The corelation coefficient plays a vital role in suggesting the best fit isotherm model.

$$\text{Sips isotherm}: q_e = Q_s \frac{K_s C_e^{n_s}}{1 + K_s C_e^{n_s}} \tag{9}$$

where Sips constants K_S $(\text{mg/L})^{-1/n}$ is the sips constant related to affinity constant, Q_s is the adsorption capacity (mg/g), and n_s corresponds to model exponent, closer to unity, indicating the adsorption process is more of Langmuir isotherm. The maximum monolayer adsorption capacity obtained was 10.23 mg/g. The separation factor, R_s (Eq. (10)) is calculated as follows:

$$R_s = Q_s \frac{1}{1 + K_s C_0^{n_s}} \tag{10}$$

This parameter indicates the type of isotherm to be irreversible ($R_s = 0$), favorable ($0 < R_s < 1$), linear ($R_s = 1$), or unfavorable ($R_s > 1$) [60]. The value of R_s was found to be 0.67, indicating the process is favorable.

Temkin isotherm (Eq. (11)) takes into account of interaction between the adsorbing species and adsorbate. Under basic assumption with the facts, (1) the heat of adsorption of all the molecules in the layer decreases linearly with coverage due to adsorbent–adsorbate interactions and then (2) the adsorption is characterized by a uniform distribution of binding energies, up to a maximum binding energy. Temkin isotherm derivation assumes that the fall in the heat of adsorption is linear rather logarithmic, as Freundlich equation is implied.

$$\text{Temkin isotherm}: q_e = B\ln(A_e) \tag{11}$$

where A corresponds to the equilibrium binding constant in relation to the maximum binding energy (L/g) and $B = (RT)/b$, b is the Temkin isotherm constant related to the heat of adsorption (J/mol), R is the universal gas constant (8.314 J/[mol K]), and T is the absolute temperature (K). The Temkin constant obtained were found to be, $A = 4.49$ and $B = 2.05$, respectively. A suitable mechanism was proposed to illustrate the interactions between the Th(IV) ion and PoU adsorbent (Fig. 11). There are two types of interactions taking place between the Th(IV) metal ion and the PoU adsorbent: (1) A direct electrostatic force of attraction creating a strong bond between the positively charged metal ions species and the electron-rich oxygen atom present in the polymeric chain linkages and (2) a coordinate bond between the oxygen and nitrogen atoms present in the polymer chain and the metal ion species. The lone pair of electrons in the oxygen and the nitrogen atom was responsible in making the coordinate bond with the metal ion species [61].

3.7. Adsorption thermodynamics

Adsorption of Th(IV) onto PoU was calculated using function of temperature and the maximum thorium removal was attained at 30°C. Thermodynamics studies were conducted at temperature ranging from 30°C, 40°C, 50°C, and 60°C for 10 mg/L of initial Th(IV) ion concentration at optimum pH 6, respectively (Fig. 12). The adsorption capacity of PoU resin decreases with constant range with increase in temperature from 30°C to 60°C [62,63]. The adsorption thermodynamic parameters were determined from the experimental data using the following equations:

$$K_d = \frac{C_{Ae}}{C_e} \tag{12}$$

$$\Delta G° = \Delta H° - \Delta S° \tag{13}$$

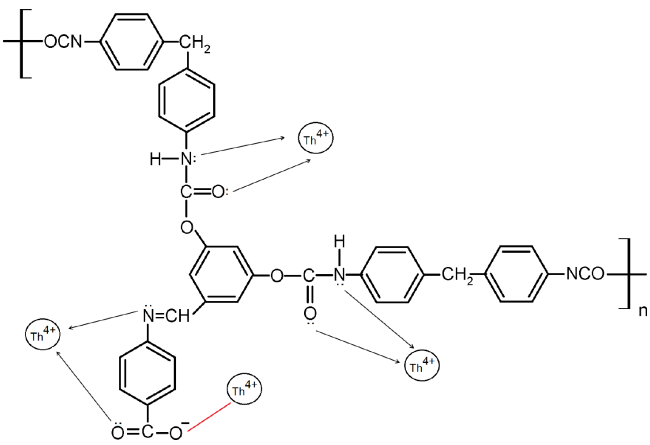

Fig. 11. Proposed mechanism of Th(IV) ion with PoU adsorbent.

$$\Delta G° = -RT\ln K_c \quad (14)$$

$$\log K_d = \frac{\Delta S°}{2.303R} - \frac{\Delta H°}{2.303RT} \quad (15)$$

where K_d is the equilibrium constant, C_e is the metal concentration at equilibrium, C_{Ae} is the amount of thorium ion adsorbed by PoU resin with per unit liter of thorium ion solution at equilibrium (mg/L). $\Delta H°$, $\Delta S°$, and $\Delta G°$ are the change in Gibbs energy (KJ/mol), change in entropy (KJ/mol), and change in enthalpy (J/mol/K), respectively, T is the absolute temperature, and R is the gas constant. From the plot of log K_d against reciprocal of temperature (1/T) (Fig. 13), the values of $\Delta H°$ and $\Delta S°$ were calculated. The other thermodynamic parameters values and constants were also calculated and tabulated (Table 3). The $\Delta G°$ value was found to be negative with proportional increase in temperature, favorable for spontaneous and feasible nature of the adsorption process in nature. The negative $\Delta H°$ value shows that the reaction is exothermic and the intensity of adsorption with temperature increase. The value of $\Delta S°$ shows more constraint on the mobility of the adsorbate molecule over PoU surface [64].

3.8. Desorption studies

Desorption studies were carried out with spent PoU adsorbent at 30°C. Because thermal activation results in 5%–10% adsorbent loss, chemical activation was carried out with Th(IV) adsorbed PoU resin. The metal adsorbed PoU resin was made in contact with eluting agents 0.1 N H_2SO_4, 0.1 N HCl, and 0.1 N CH_3COOH separately. The solution was centrifuged and concentration was calculated with UV-Visible spectrophotometer. The percentage of desorption was calculated using Eq. (16):

$$\text{Th(IV) desorbed } \% = \frac{R_d}{R_a} \times 100 \quad (16)$$

where R_d and R_a correspond to amount of Th(IV) desorbed by elutant (mg/g) and amount of Th(IV) adsorbed by PoU resin (mg/g). From the results, it was evident that PoU resin was found to be stable up to five cycles with mere changes in the adsorption–desorption ratio shown in Fig. 14.

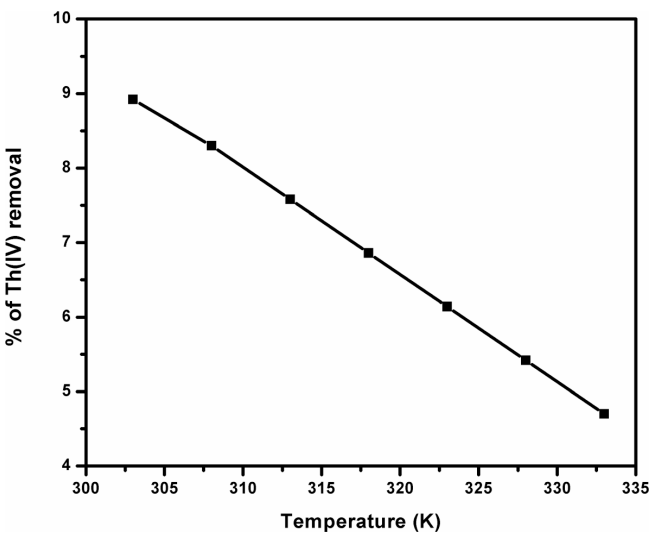

Fig. 12. Temperature studies of Th(IV) removal by PoU adsorbent.

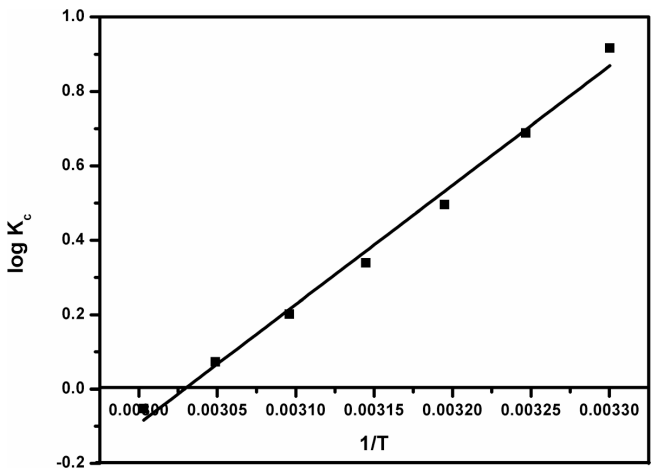

Fig. 13. Thermodynamic studies of Th(IV) removal by PoU adsorbent.

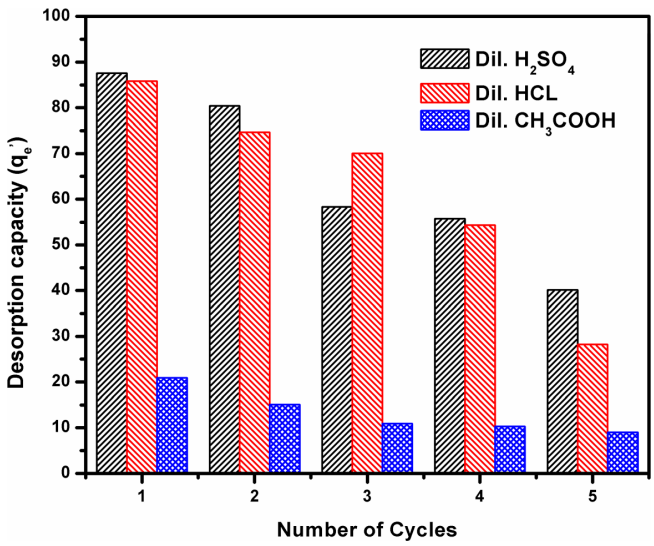

Fig. 14. Desorption studies of PoU adsorbent with elutants at 30°C.

Table 3
Thermodynamic parameter and constants for Th(IV) removal by PoU adsorbent

ΔH	ΔS	ΔG (kJ.mol^{-1})						
(kJ.mol^{-1})	(Jk^{-1}.mol^{-1})	303 K	308 K	313 K	318 K	323 K	328 K	333 K
–61.34	–185.80	–20.80	–12.50	–8.15	–5.77	–4.27	–3.22	–2.45

Table 4
Comparison of Th(IV) removal by PoU resin with other reported adsorbents

Polymeric adsorbents	Th(IV) removal q_e (mg.g^{-1})	Reference
Perlite	5.8	[6]
Cellulose composite	21.3	[9]
Poly(amido)amine dendron-functionalized styrene diviyl benzene	36.2	[2]
Poly(ethylene oxide) and poly(L-lactide) fibrous membranes	50.1	[65]
Titan yellow-impregnated polystyrene-divinyl benzene copolymer-7 resin beads	1.5	[66]
Polyurethane (PoU)	8.93	Present study

The adsorption–desorption experiment illustrated effective performance of the PoU resin in consecutive cycles with strong chemical stability nature with no serious performance decline. A comparison table was charted to compare the adsorption capacity of PoU resin with other reported adsorbent, among them PoU resin showed good adsorption performance (Table 4). The table clearly states that a donor–acceptor polymer containing chelating functional group can effectively take part in the adsorption process, and it can effectively remove even the trace amount of metal ions from wastewater effluent.

4. Conclusion

In this study, the adsorption of Th(IV) from aqueous solutions by PoU as a function of contact time, solution pH, concentration of ions, and temperature was investigated. Based on the observed data, following conclusions are obtained: Maximum removal of Th(IV) by PoU resin was observed at pH 5.5. The Freundlich isotherm constant, K_F and n values were found to be 11.34 (mg/g)(L/mg)(1/n) and 2.25 g/L for the thorium removal by PoU adsorbent suggesting that the rate limiting step involves more than one mechanism and follows pseudo-second-order kinetic model. The negative ΔG value shows the reaction is more feasible and spontaneous. The negative ΔS and ΔH values indicate the affinity between PoU resin and Th(IV) ion interface and exothermic nature of the system. Repeated adsorption–desorption experiments showed that the PoU resin has potential application in the removal and recovery of Th(IV) ions in aqueous media.

References

[1] P. Ilaiyaraja, A.K.S. Deb, K. Sivasubramanian, D. Ponraju, B. Venkatraman, Adsorption of uranium from aqueous solution by PAMAM dendron-functionalized styrene divinylbenzene, J. Hazard. Mater., 250 (2013) 155–166.

[2] P. Ilaiyaraja, A.K.S. Deb, K. Sivasubramanian, D. Ponraju, B. Venkatraman, Removal of thorium from aqueous solution by adsorption using PAMAM dendron-functionalized styrene divinyl benzene, J. Radioanal. Nucl. Chem., 297 (2013) 59–69.

[3] T.S. Anirudhan, S.R. Rejeena, Thorium(IV) removal and recovery from aqueous solutions using tannin-modified poly(glycidylmethacrylate)-grafted zirconium oxide densified cellulose, Ind. Eng. Chem. Res., 50 (2011) 13288–13298.

[4] M. Metaxas, V. Kasselouri-Rigopoulo, P. Galiatsatou, C. Konstantopoulou, D. Oikonomou, Thorium removal by different adsorbents, J. Hazard. Mater., 97 (2003) 71–82.

[5] D. Baybas, U. Ulusoy, The use of polyacrylamide-aluminosilicate composites for thorium adsorption, Appl. Clay Sci., 51 (2011) 138–146.

[6] Z. Talip, M. Eral, U. Hicsonmez, Adsorption of thorium from aqueous solutions by perlite, J. Environ. Rad., 100 (2009) 139–143.

[7] T.S. Anirudhan, L. Divya. P.S. Suchitra, Kinetic and equilibrium characterization of uranium(VI) adsorption onto carboxylate-functionalized poly(hydroxyethylmethacrylate)-grafted lignocellulosics, J. Environ. Manage., 90 (2009) 549–560.

[8] T.S. Anirudhan, C.D. Bringle, S. Rijith, Removal of uranium (VI) from aqueous solutions and nuclear industry effluents using humic acid-immobilized zirconium-pillared clay, Desal. Wat. Treat., 12 (2009) 16–27.

[9] P.D. Bhalara, D. Punetha, K. Balasubramanian, Kinetic and isotherm analysis for selective thorium(IV) retrieval from aqueous environment using eco-friendly cellulose composite, Int. J. Environ. Sci. Technol., 12 (2015) 3095–3106.

[10] G. Sharma, M. Naushad, A.H. Al-Muhtaseb, A. Kumar, M.R. Khan, S. Kalia, Shweta, M. Bala, A. Sharma, Fabrication and characterization of chitosan-crosslinked-poly(alginic acid) nanohydrogel for adsorptive removal of Cr(VI) metal ion from aqueous medium, Int. J. Biol. Macromol., 95 (2017) 484–493.

[11] Z.A. Alothman, M.M. Alam, M. Naushad, Heavy toxic metal ion exchange kinetics: validation of ion exchange process on composite cation exchanger nylon 6,6 Zr(IV) phosphate, J. Ind. Eng. Chem., 19 (2013) 956–960.

[12] P. Rule, K. Balasubramanian, R.R. Gonte, Uranium(VI) remediation from aqueous environment using impregnated cellulose beads, J. Environ. Rad., 136 (2014) 22–29.

[13] M. Naushad, Z.A. Alothman, M.R. Awual, M.M. Alam, G.E. Eldesoky, Adsorption kinetics, isotherms and thermodynamic studies for the adsorption of Pb^{2+} and Hg^{2+} metal ions from aqueous medium using Ti(IV) iodovanadate cation exchanger, Ionics, 21 (2015) 2237–2245.

[14] Z.A. Alothman, Inamuddin, M. Naushad, Adsorption thermodynamics of trichloroacetic acid herbicide on polypyrrole Th(IV) phosphate composite cation-exchanger, Chem. Eng. J., 169 (2011) 38–42.

[15] A. Rahmati, A. Ghaemi, M. Samadfam, Kinetic and thermodynamic studies of uranium(VI) adsorption using Amberlite IRA-910 resin, Ann. Nucl. Energy, 39 (2012) 42–48.

[16] A.K. Kaygun, S. Akyil, Study of the behaviour of thorium adsorption on PAN/zeolite composite adsorbent, J. Hazard. Mater., 147 (2007) 357–362.

[17] Z.J. Guo, X.M. Yu, F.H. Guo, Z.Y. Tao, Th(IV) adsorption on alumina: effects of contact time, pH, ionic strength and phosphate, J. Colloid Interface Sci., 288 (2005) 14–20.

[18] C. Kutahyali, M. Eral, Sorption studies of uranium and thorium on activated carbon prepared from olive stones: kinetic and thermodynamic aspects, J. Nucl. Mater., 396 (2010) 251–256.

[19] D.L. Guerra, R.R. Viana, C. Airoldi, Adsorption of thorium cation on modified clays MTTZ derivative, J. Hazard. Mater., 168 (2009) 1504–1511.

[20] R. Qadeer, J. Hanif, I. Hanif, Uptake of thorium ions from aqueous solutions by a molecular sieve (13X type) powder, J. Radioanal. Nucl. Chem., 190 (1995) 103–112.

[21] O. Ozay, S. Ekici, N. Aktas, N. Sahiner, P(4-vinyl pyridine) hydrogel use for the removal of UO_2^{2+} and Th^{4+} from aqueous environments, J. Environ. Manage., 92 (2011) 3121–3129.

[22] G. Sharma, D. Pathania, M. Naushad, Preparation, characterization, and ion exchange behavior of nanocomposite polyaniline zirconium(IV) selenotungstophosphate for the separation of toxic metal ions, Ionics, 21 (2015) 1045–1055.

[23] V.K. Jain, A. Handa, S.S. Sait, P. Shrivastav, Y.K. Agrawal, Pre-concentration, separation and trace determination of lanthanum(III), cerium(III), thorium(IV) and uranium(VI) on polymer supported o-vanillinsemicarbazone, Anal. Chim. Acta, 429 (2001) 237–246.
[24] P. Metilda, J.M. Gladis, T.P. Rao, Quinoline-8-ol modified cellulose as solid phase extractant (SPE) for preconcentrative separation and determination of thorium(IV), Radiochim. Acta, 91 (2003) 737–741.
[25] V.K. Jain, R.A. Pandya, S.G. Pillai, P.S. Shrivastav, Simultaneous preconcentration of uranium(VI) and thorium(IV) from aqueous solutions using a chelating calix[4]arene anchored chloromethylated polystyrene solid phase, Talanta, 70 (2006) 257–266.
[26] C.S.K. Raju, M.S. Subramanian, Selective preconcentration of U(VI) and Th(IV) in trace and macroscopic levels using malonamide grafted polymer from acidic matrices, Microchim. Acta, 150 (2005) 297–304.
[27] A. Murugesan, L. Ravikumar, V. Sathyaselvabala, P. Senthilkumar, T. Vidhyadevi, S.D. Kirupha, S.S. Kalaivani, S. Krithiga, S. Sivanesan, Removal of Pb (II), Cu (II) and Cd (II) ions from aqueous solution using polyazomethineamides: equilibrium and kinetic approach, Desalination, 271 (2011) 199–208.
[28] S.D. Kirupha, R. Narayansamy, M. Sornalatha, S. Sivanesan, L. Ravikumar, Synthesis and metal ion uptake studies of chelating polyurethane resin containing donor atoms: experimental optimization and temperature studies, Can. J. Chem. Eng., 95 (2017) 944–953.
[29] S.D. Kirupha, S. Kalaivani, T. Vidhyadevi, P. Premkumar, P. Baskaralingam, S. Sivanesan, L. Ravikumar, Effective removal of heavy metal ions from aqueous solutions using a new chelating resin poly [2,5-(1,3,4-thiadiazole)-benzalimine]: kinetic and thermodynamic study, J. Water Reuse Desal., 6 (2016) 310–324.
[30] D. Pathania, G. Sharma, M. Naushad, A. Kumar, Synthesis and characterization of a new nanocomposite cation exchanger polyacrylamide Ce(IV) silicophosphate: photocatalytic and antimicrobial applications, J. Ind. Eng. Chem., 20 (2014) 3596–3603.
[31] D. Pathania, D. Gupta, N.C. Kothiyal, G. Sharma, G.E. Eldesoky, M. Naushad, Preparation of a novel chitosan-g-poly(acrylamide)/Zn nanocomposite hydrogel and its applications for controlled drug delivery of ofloxacin, Int. J. Biol. Macromol., 84 (2016) 340–348.
[32] M. Naushad, T. Ahamad, B.M. Al-Maswari, A.A. Alqadami, S.M. Alshehri, Nickel ferrite bearing nitrogen-doped mesoporous carbon as efficient adsorbent for the removal of highly toxic metal ion from aqueous medium, Chem. Eng. J., 330 (2017) 1351–1360.
[33] K. Anbalagan, P.S. Kumar, K.S. Gayatri, S.S. Hameed, M. Sindhuja, C. Prabhakaran, R. Karthikeyan, Removal and recovery Ni(II) ions from synthetic wastewater using surface modified Strychnos potatorum seeds: experimental optimization and Mechanism, Desal. Wat. Treat., 53 (2015) 171–182.
[34] U.P. Kiruba, P.S. Kumar, K.S. Gayatri, S.S. Hameed, M. Sindhuja, C. Prabhakaran, Study of adsorption kinetic, mechanism, isotherm, thermodynamic and design models for Cu(II) ions on sulphuric acid modified Eucalyptus seeds: temperature effect, Desal. Wat. Treat., 56 (2015) 2948–2965.
[35] D. Prabu, R. Parthiban, P.S. Kumar, N. Kumari, P. Saikia, Adsorption of copper ions onto nano scale zero-valent iron impregnated cashew nut shell, Desal. Wat. Treat., 57 (2016) 6487–6502.
[36] K. Anbalagan, P.S. Kumar, R. Karthikeyan, Adsorption of toxic Cr(VI) ions from aqueous solution by sulphuric acid modified *Strychnos potatorum* seeds in batch and column studies, Desal. Wat. Treat., 57 (2016) 12585–12607.
[37] N.T. Abdel-Ghani, M. Hefray, G.A.F. El-Chaghaby, Removal of lead from aqueous solution using low cost abundantly available adsorbents, Int. J. Environ. Sci. Technol., 4 (2007) 67–73.
[38] T. Anitha, P.S. Kumar, K.S. Kumar, K. Sriram, J.F. Ahmed, Biosorption of lead(II) ions onto nano-sized chitosan particle blended polyvinyl alcohol (PVA): adsorption isotherms, kinetics and equilibrium studies, Desal. Wat. Treat., 57 (2016) 13711–13721.
[39] A. Saravanan, P.S. Kumar, B. Preetha, Optimization of process parameters for the removal of chromium(VI) and nickel(II) from aqueous solutions by mixed biosorbents (custard apple seeds and *Aspergillus niger*) using response surface methodology, Desal. Wat. Treat., 57 (2016) 14530–14543.
[40] P. Rajkumar, P.S. Kumar, S.D. Kirupha, T. Vidhyadevi, J. Nandagopal, S. Sivanesan, Adsorption of Pb(II) ions onto surface modified *Guazuma ulmifolia* seeds and batch adsorber design, Environ. Prog. Sustainable Energy, 32 (2013) 307–316.
[41] S. Suganya, K. Kayalvizhi, P.S. Kumar, A. Saravanan, V.V. Kumar, Biosorption of Pb(II), Ni(II) and Cr(VI) ions from aqueous solution using *Rhizoclonium tortuosum*: extended application to nickel plating industrial wastewater, Desal. Wat. Treat., 57 (2016) 25114–25139.
[42] A. Saravanan, P.S. Kumar, M.Yashwanthraj, Sequestration of toxic Cr(VI) ions from industrial wastewater using waste biomass: a review, Desal. Wat. Treat., 68 (2017) 245–266.
[43] R. Gayathri, K.P. Gopinath, P.S. Kumar, A. Saravanan, Antimicrobial activity of *Mukia maderasapatna* stem extract of jujube seeds activated carbon against gram-positive/gram-negative bacteria and fungi strains: application in heavy metal removal, Desal. Wat. Treat., 72 (2017) 418–427.
[44] K. Nithya, A. Sathish, P.S. Kumar, T. Ramachandran, An insight into the prediction of biosorption mechanism, and isotherm, kinetic and thermodynamic studies for Ni(II) ions removal from aqueous solution using acid treated bio-sorbent: the *Lantana camara* fruit, Desal. Wat. Treat., 80 (2017) 276–287.
[45] G. Padmalaya, B.S. Sreeja, P.S. Kumar, M. Arivanandhan, Chitosan anchored zinc oxide nanocomposite as modified electrochemical sensor for the detection of Cd (II) ions, Desal. Wat. Treat., 97 (2017) 295–303.
[46] K. Nithya, A. Sathish, P.S. Kumar, T. Ramachandran, Fast kinetics and high adsorption capacity of green extract capped superparamagnetic iron oxide nanoparticles for the adsorption of Ni(II) ions, J. Ind. Eng. Chem., 59 (2018) 230–241.
[47] D. Prabu, R. Parthiban, P.S. Kumar, A. Saravanan, R. John, T. Titus, Sorption of Cu(II) ions by nano-scale zero valent iron supported on rubber seed shell, IET Nanobiotechnol., 11 (2017) 714–724.
[48] S. Lagergren, About the theory of so-called adsorption of soluble substances, K. Sven. Vetensk. Akad. Handl., 24 (1898) 1–39.
[49] T.S. Anirudhan, P.G. Radhakrishnan, K. Vijayan, Development of a first-order kinetics based model, equilibrium studies, and thermodynamics for the adsorption of methyl orange onto a lignocellulosic anion exchanger, Sep. Sci. Technol., 48 (2013) 947–959.
[50] A. Frost, R. Pearson, Kinetics and mechanism, second edition, J. Phys. Chem., 65 (1961) 384.
[51] Y.S. Ho, G. Mckay, Pseudo-second order model for sorption processes, Process Biochem., 34 (1999) 451–465.
[52] R.R. Gonte, G. Shelar, K. Balasubramanian, Polymer–agro-waste composites for removal of Congo red dye from wastewater: adsorption isotherms and kinetics, Desal. Wat. Treat., 52 (2014) 7797–7811.
[53] W.J. Weber, J.C. Morris, Kinetics of adsorption carbon from solutions, J. Sanit. Eng. Div. Am. Soc. Civil Eng., 89 (1963) 31–60.
[54] I. Langmuir, The adsorption of gases on plane surfaces of glass, mica and platinum, J. Am. Chem. Soc., 40 (1918) 1361–1403.
[55] H.M.F. Freundlich, Over the adsorption in solution, J. Phys. Chem., 57 (1906) 385.
[56] R.J. Umpleby, S.C. Baxter, Y. Chen, R.N. Shah, K.D. Shimizu, Characterization of molecularly imprinted polymers with the Langmuir-Freundlich isotherm, Anal. Chem., 73 (2001) 4584–4591.
[57] M.J. Temkin, V. Pyzhev, Recent modifications to Langmuir isotherms, Acta Physicochim., 12 (1940) 217–225.
[58] P.S. Kumar, S. Ramalingam, V. Sathyaselvabala, S.D. Kirupha, S. Sivanesan, Removal of copper(II) ions from aqueous solution by adsorption using cashewnut shell, Desalination, 266 (2011) 63–71.

[59] P.S. Kumar, S. Ramalingam, S.D. Kirupha, A. Murugesan, T. Vidhyadevi, S. Sivanesan, Adsorption behavior of nickel(II) onto cashew nut shell: equilibrium, thermodynamics, kinetics, mechanism and process design, Chem. Eng. J., 167 (2011) 122–131.
[60] A. Gunay, E. Arslankaya, I. Tosun, Lead removal from aqueous solution by natural and pretreated clinoptilolite: adsorption equilibrium and kinetics, J. Hazard. Mater., 146 (2007) 362–371.
[61] A.A. Alqadami, M. Naushad, Z.A. Alothman, A.A. Ghfar, Novel metal–organic framework (MOF) based composite material for the sequestration of U(VI) and Th(IV) metal ions from aqueous environment, ACS Appl. Mater. Interfaces, 41 (2017) 36026–36037.
[62] K. Bannerjee, G.L. Amy, M. Prevost, S. Nour, M. Jekel, P.M. Gallagher, C.D. Blumenschein, Kinetic and thermodynamic aspects of adsorption of arsenic onto granular ferric hydroxide (GFH), Water Res., 42 (2008) 3371–3378.
[63] L.D. Michelson, P.G. Gideon, E.G. Pace, L.H. Kutal, Removal of solute mercury from wastewater by a complexing technique, US Dept. Industry Off. Water Res. Technol., 74 (1975) 25.
[64] P.S. Kumar, S. Ramalingam, R.V. Abhinaya, S.D. Kirupha, A. Murugesan, S. Sivanesan, Adsorption of metal ions onto the chemically modified agricultural waste, Clean, 40 (2012) 188–197.
[65] I. Savva, M. Efstathiou, T. Krasia-Christoforou, I. Pashalidis, Adsorptive removal of. U(VI) and Th(IV) from aqueous solutions using polymer-based electrospun PEO/PLLA fibrous membranes, J. Radioanal. Nucl. Chem., 298 (2013) 1991–1997.
[66] H.U. Kaynar, M. Ayvacikli, U. Hicsonmez, S.C. Kaynar, Removal of thorium (IV) ions from aqueous solution by a novel nanoporous ZnO: isotherms, kinetic and thermodynamic studies, J. Environ. Radioact., 150 (2015) 145–151.